

# Hydrocarbon radicals interaction with amorphous carbon surfaces

A.R. Sharma<sup>a</sup>, R. Schneider<sup>a,\*</sup>, U. Toussaint<sup>b</sup>, K. Nordlund<sup>c</sup>

<sup>a</sup> Max-Planck-Institut für Plasmaphysik, Teilinstitut Greifswald, EURATOM Association, D-17491 Greifswald, Germany

<sup>b</sup> EURATOM Association, Max-Planck-Institut für Plasmaphysik, Boltzmannstr. 2, D-85748 Garching, Germany

<sup>c</sup> Accelerator Laboratory, University of Helsinki, P.O. Box 43, FIN-00014, Finland

## Abstract

Total reflection coefficients and break-up patterns for incident atomic carbon, C<sub>2</sub>, CH, CH<sub>2</sub>, CH<sub>3</sub>, CH<sub>4</sub>, C<sub>2</sub>H, C<sub>2</sub>H<sub>2</sub>, C<sub>2</sub>H<sub>3</sub>, C<sub>2</sub>H<sub>4</sub>, C<sub>2</sub>H<sub>5</sub> and C<sub>2</sub>H<sub>6</sub> from an amorphous hydrocarbon surface with a H:C ratio of 0.66 are calculated using the HCParcas molecular dynamics code with an empirical Brenner potential. Incident molecules are separately equilibrated at incident energies ranging from thermal up to the maximum energies at which the molecules can be structurally stabilized to mimic the conditions in an equilibrium plasma.

© 2007 Elsevier B.V. All rights reserved.

PACS: 34.50.Dy; 52.40.Hf; 31.15.Qg; 34.50.–s

Keywords: Amorphous carbon; Co-deposition; Erosion and deposition; Hydrocarbons; Molecular dynamic simulations

## 1. Introduction

Hydrocarbon formation, transformation and deposition is a crucial problem for fusion devices [1]. The Co-deposited layers, referred to the carbon and hydrocarbon layers deposited beyond the diverter and not in direct contact with the plasma, remain a serious issue due to hydrogen isotope retention in these layers [2]. Co-deposited layers with varying thickness have been observed in major machine operations, such as JET [3], TEXTOR [4] and ASDEX Upgrade [5–8]. Small-scale experiments have been performed to study the transport

and deposition of hydrocarbons in a stationary plasma. One such experimental device is PSI-2 in which in situ measurements on film growth for different plasma parameters [9,10] were performed. The transport of injected gas molecules and the growth rates of the CH-film in PSI-2 were simulated with the 3D Monte Carlo code ERO [11] using three different reaction rate coefficients [12–15]. However, the observed deposition rates in the experiments [10] are much higher than the values obtained by the ERO code [16]. A possible explanation for this discrepancy is the inaccuracy of the sticking coefficient data used in the ERO modeling. Presumably the energy dependence of the sticking coefficients plays an important role in predicting the right deposition rates.

\* Corresponding author.

E-mail address: [Ralf.Schneider@ipp.mpg.de](mailto:Ralf.Schneider@ipp.mpg.de) (R. Schneider).

## 2. Modeling

The HCParcas molecular dynamics code with the empirical Brenner potential [17] for hydrogen carbon interaction was used in the present study. Potential cutoff of 2.0 Å for carbon–carbon interaction was used in the present calculation. High accuracy tight binding molecular dynamics simulations to calculate the sticking of molecules are computationally expensive and only suited for smaller systems [18].

An amorphous structure was prepared by starting with a random arrangement of hydrogen and carbon atoms (986 atoms in total) with a H:C-ratio of 0.66 with periodic boundary conditions in three-dimensions. We applied four cycles of heating up to 3000 K and subsequent cooling down to 200 K, to avoid local minima in the initial configuration. Switching to periodic boundary conditions only in the  $x$ - and  $y$ -directions and slowly heating to 300 K was followed by very long runs (300 ns) for relaxation in the  $z$ -direction. This allows for sample preparation with a relaxed surface in the  $z$ -direction, to avoid artificial sputtering of atoms and molecules from the surface due to the relaxation of the surface rather than due to impinging molecules/radicals.

The incident hydrocarbon molecules and radicals studied in the present work are separately equilibrated for energies of the incident particles up to a maximum energy at which the molecule/radical are structurally stable. The equilibrated energy is the average kinetic energy of the incident molecules. This procedure allows the molecules to have rotational and vibrational degrees of freedom as they approach the sample surface. This approach represents the true physical picture as there are no means in the PSI-2 experiments to suppress the rotational–vibrational excitations. It is also known that the total energy gained by the molecules in the plasma would have translational, rotational and vibrational contributions [19–25]. Spectroscopic measurements of the vibrational states have been made in TEXTOR [19]. Also the distribution of the  $H_2$  molecules within the many vibrational levels of the electronic ground state has been studied theoretically [20,21] and experimentally [22–25]. Equilibration of the molecule/radical at the desired incident energy poses the limit to which the molecules can be accelerated. We observe that at higher energies the molecules/radicals become structurally unstable and dissociate before approaching the surface. For a non-rotating linear molecule, such as CH, with

translational freedom along the  $z$ -axis, vibrational modes are excited along the translational direction of motion. At higher energies, the vibrational amplitude are high enough to knock-off the lower mass hydrogen atom by the heavier carbon atom, thus dissociating the molecule. Structural instability is more pronounced in molecules such as  $C_2H_3$  and  $C_2H_5$  where hydrogen atoms are known to be ‘floppy’ [26–28].

The starting position coordinates for the molecules and radicals are sampled uniformly over the surface and rotational freedom allows to sample all possible interaction configurations. This is specially important for linear molecules such as CH,  $C_2H$  and  $C_2H_2$  which otherwise would approach the surface at fixed orientations.

Alaman and Ruzic have already performed a similar molecular dynamics studies to calculate the reflection and dissociation coefficients of hydrocarbons [29]. However, the surface used in their work Ref. [29] was prepared by bombarding a graphite lattice with hydrogen atoms, which leaves lattice planes at every depth in the sample. Such surfaces can be compared with plasma-exposed surfaces [29], which are typical for carbon divertor target plates. The hard and soft surface in Ref. [29] have an average H to C ratio of 0.42 and 0.4 respectively, which differs significantly from the H to C ratio of 0.66, used in the present work. This H to C ratio represents a Co-deposited layer in fusion devices and is much softer than the surface used in Ref. [29]. Fig. 1 shows the hydrogen to carbon ratio of

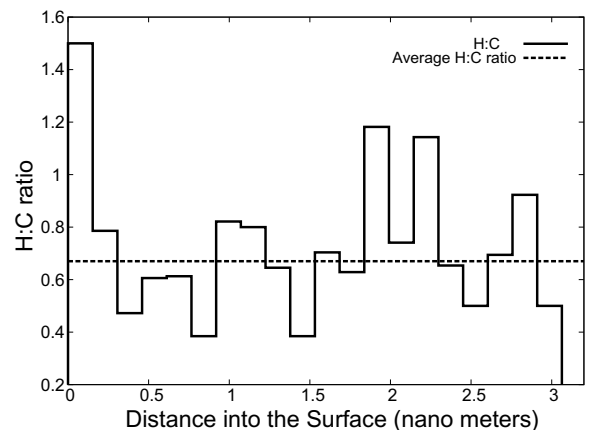


Fig. 1. Depth profile showing H to C ratio as a function of distance into the surface.  $Z = 0$ ; refers to the surface atoms. Bin width = 1.532 Å.

the prepared sample as a function of the distance from the surface into the sample.

### 3. Results and discussion

#### 3.1. Reflection coefficients

The reflection coefficients for atomic carbon, molecules/radicals such as  $C_2$ ,  $CH$ ,  $CH_2$ ,  $CH_3$ ,  $CH_4$ ,  $C_2H$ ,  $C_2H_2$ ,  $C_2H_3$ ,  $C_2H_4$ ,  $C_2H_5$  and  $C_2H_6$  incident on the above described sample are reported in this section. In the present work, the reflection coefficient for a given species is defined as the ratio of the number of reflected atoms or molecules of this species to the number of incident molecules/radicals. In case of  $C_2H_x$  incidence, the total carbon reflection coefficient is calculated by summing-up the partial reflection coefficients of  $C_2H_x$  reflected species and one-half of the  $CH_x$  reflection coefficients. For the sake of clarity, statistical uncertainty in the calculated reflection coefficient is shown only for selected species.

Here the influence of the rotational freedom of the incident molecule on the reflection coefficient from the amorphous hydrocarbon surface has to be considered. Non-rotating hetero-nuclear linear molecule (e.g.  $CH$ ) impinging on the surface can have many possible orientations with respect to the normal of the surface. Two extreme orientations for  $CH$  are with C down (i.e. the bond axis for the molecule is parallel to the normal to the surface and the molecule approaches the surface with the carbon atom towards and the hydrogen atom away from the surface) and H down (i.e. the hydrogen atom is towards the surface and the carbon atom is positioned away from the surface). It can be seen from Fig. 2 that the reflection coefficient for the case with C down is lower (higher sticking) than the case with H down. Higher carbon sticking is favoured due to open carbon bonded chains at the surface which act as trap sites for carbon bonding. Also higher concentration of hydrogen on the surface contributes to higher reflection in the case of the H down orientation. The region between the upper and lower curve gives an estimate of the spread in the reflection coefficient due to various possible orientations at the time of molecule impact. The average reflection coefficient of a rotating  $CH$  molecule incident on the surface is expected to lie within the band with a possible deviation due to statistical errors.

Fig. 3 shows the energy dependence of reflection coefficients for atomic carbon and  $C_2$  incident on an

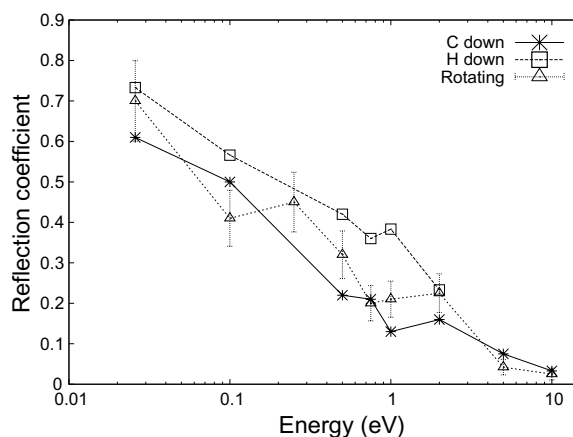


Fig. 2. Spread in reflection coefficient due to different orientation of  $CH$  incidence.

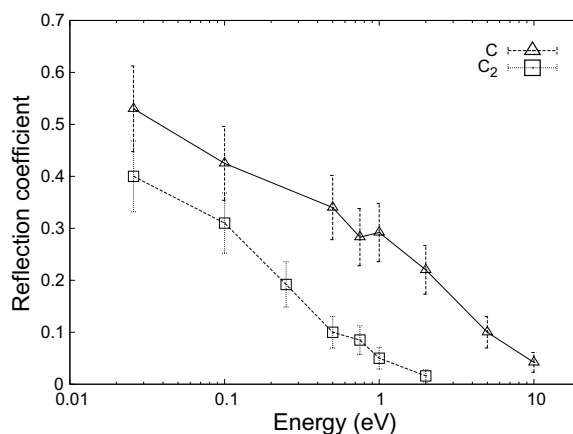


Fig. 3. Reflection coefficient for atomic carbon and carbon dimer. For  $C_2$ , the bond axis of the molecule is parallel to the normal to the surface.

amorphous hydrocarbon surface for normal incidence. Normal incidence was chosen as there is no known angular dependence of the reflection coefficient as a function of incident energy [29]. The calculated reflection coefficients of 0.43 at thermal energies and 0.042 at 10 eV for atomic carbon reflection, compared with Ref. [29] are lower by 10–17%, respectively, but show the same general trends. This difference in the reflection coefficients is attributed to the higher H to C ratio in the surface layer used in the present calculations, which makes the surface softer compared with the surface used in Ref. [29]. A softer surface allows for deeper penetration into the surface, thus increasing the sticking probability. The probability of hydrogen release during  $C_2$  bombardment from the surface increases from less than 1% at

5 eV to 15% at 10 eV. The probability of complex hydrocarbon release at 10 eV is less than 1%.

Similar to the above observation, the  $C_2$  reflection coefficient of 0.4 (Fig. 3) at thermal energy is lower than the value of 0.5, and follows the same decreasing trend as reported in Ref. [29]. However,  $C_2$  shows a high probability for hydrogen capture from the surface, thus strongly lowering its reflection probability as explained in more detail in Section 3.4.

### 3.2. Reflection coefficients for $CH_x$ ( $x = 1-4$ )

In Fig. 4, we present the reflection coefficients of CH,  $CH_2$ ,  $CH_3$  and  $CH_4$  as a function of energy. The general trend shows that the reflection coefficient decreases with increasing energy.  $CH_4$  shows a 100% probability of reflection up to 0.75 eV. In the energy range between 2 and 5 eV all molecules show a decrease in reflection coefficients. This can be explained by studying the break-up pattern of these molecules, discussed in Section 3.4.

### 3.3. Reflection coefficients for $C_2H_x$ ( $x = 1-6$ )

Reflection coefficients for  $C_2H_x$  ( $x = 1-6$ ) presented in Fig. 5 show that they are higher for molecules with an even number of hydrogen atoms compared to those with an odd number. This is expected, as hydrocarbons with an odd number of hydrogen atoms are radicals and have higher reactivity with surface atoms.

$C_2H_2$ ,  $C_2H_4$  and  $C_2H_6$  show 100% chance of reflection from thermal to 0.5 eV energy range.

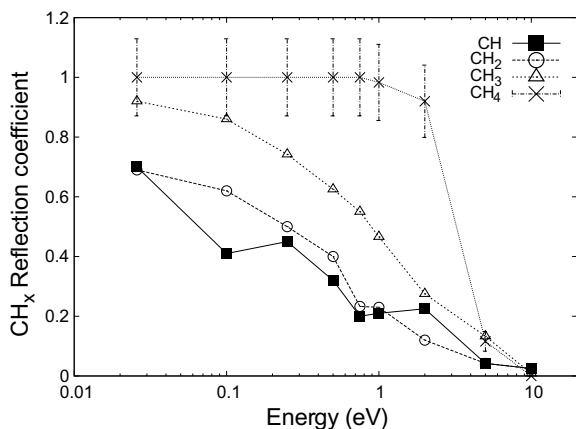


Fig. 4. Reflection coefficient for  $CH_x$  ( $x = 1-4$ ) bombardment on amorphous hydrocarbon surface.

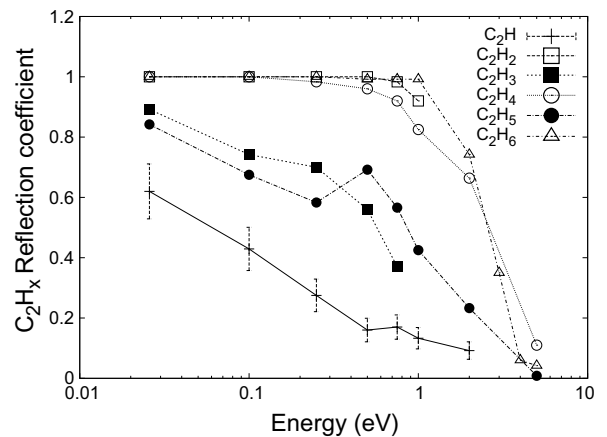


Fig. 5. Reflection coefficient for  $C_2H_x$  ( $x = 1-6$ ) bombardment on amorphous hydrocarbon surface.

The reflection of  $C_2H_2$  decreases marginally to 92% at 1 eV. Beyond 1 eV the reflection of  $C_2H_6$  and  $C_2H_4$  rapidly decreases with increasing energy. The decrease in the reflection coefficient can be partly attributed to higher sticking. The other factor responsible for the decrease is the reflection of the incident molecule in modified hydrocarbon forms due to hydrogen/carbon capture/dissociation. Radicals, such as  $C_2H$ ,  $C_2H_3$  and  $C_2H_5$  show a steep drop of the reflection coefficient due to their higher reactivity with the surface atoms.  $C_2H_3$  is known to have a ‘floppy’ structure with the hydrogen atoms tunneling between two carbon atoms [26,27]. This molecule has a low threshold for hydrogen dissociation and hence can not be stabilized at higher energies than 1.0 eV. The reflection probability for  $C_2H_3$  decreases from 90% at thermal energy to 37% at 0.75 eV.

### 3.4. Break-up pattern

The decrease in the reflection coefficient of the incident molecules/radicals as seen in Figs. 4 and 5 can be explained by studying the break-up pattern in the hydrocarbon reflection process. As an example, shown in Fig. 6, the reflection coefficient and break-up pattern for  $C_2H_6$  is discussed. The  $C_2H_6$  molecule shows 100% reflection up to an energy of 1 eV with no secondary hydrocarbon sputtering.  $H_2$  release observed over the entire energy range is due to the release of weakly bonded hydrogen atoms in the sample. Surface relaxation triggers the release of such atoms and is not a consequence of direct

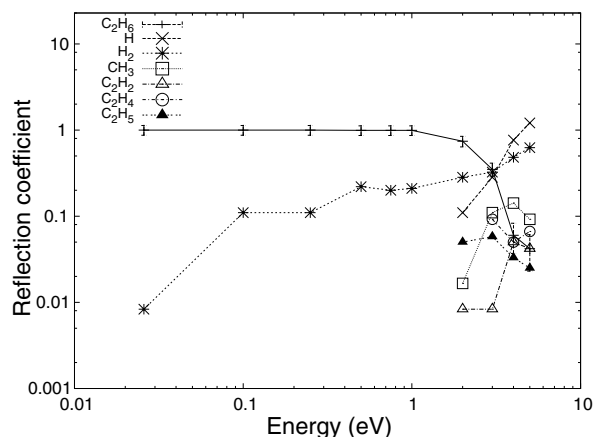


Fig. 6. Break-up pattern for  $C_2H_6$  bombardment on amorphous hydrocarbon surface.

chemical interaction. Secondary sputtering of  $H_2$  molecules will be different for other calculations, as the surface prepared with different methods and a different H to C ratio will relax differently. Above 1 eV energy, other than the incident  $C_2H_6$  reflection, the most probable mechanism is the reflection of  $C_2H_5$  where one H bond (CH bond energy 4.3 eV) is likely to be broken with a probability of 2.5%. At 5 eV, two hydrogen atoms are likely to be stripped off the incident molecule, resulting in a 4.2% chance of  $C_2H_2$  reflection. The carbon–carbon bond dissociation (C–C bond energy in ethane = 3.94 eV) has a probability of 9.2% which results in the increased release of  $CH_3$  at 5 eV.

Atomic carbon, incident on the surface is either purely reflected as atomic carbon or absorbed at the surface. Above 5 eV incident energy, the energy dumped by the incident atom/molecule supported by higher H to C ratio in surface layer (Fig. 4) favours sputtering of hydrogen atoms from the surface.

Carbon dimer and  $CH_x$  ( $x = 1-4$ ) are purely reflected below 0.75 eV. Around 1 eV, there is an increased probability for  $C_2$ , CH,  $CH_2$  and  $CH_3$  to capture a hydrogen atom from the surface due to the large number of available hydrogen atoms on the surface layer. However, in case of  $CH_4$  incidence, the probability to strip one hydrogen atom from the incident molecule and reflect as  $CH_3$ , increases from 2.5% at 2 eV incident energy to 12.5% at 5 eV. Above 1 eV more complex hydrocarbons with two or three carbon atoms are released from the surface.  $C_2H_x$  ( $x = 1-6$ ) show similar distribution in reflected molecules. General trends observed in the break-up pattern for C,  $C_2$ ,  $CH_x$

( $x = 1-4$ ) and  $C_2H_x$  ( $x = 1-6$ ) are presented in more detail in Ref. [30].

#### 4. Conclusion

The reflection coefficients of atomic carbon,  $C_2$ , CH,  $CH_2$ ,  $CH_3$ ,  $CH_4$ ,  $C_2H$ ,  $C_2H_2$ ,  $C_2H_3$  and  $C_2H_4$  show a decreasing trend with increasing energy. This trend in the reflection coefficient also holds for surfaces with H to C different than 0.66 [29]. However, numerical values of the reflection coefficient and reflection break-up pattern is sensitive to the hydrogen and carbon stacking in the sample surface.

Reflection coefficient for  $CH_x$  ( $x = 1-4$ ) increases with increasing number of hydrogen atoms. At energies above 1 eV these molecules have a higher probability to either capture a hydrogen atom from the surface or to break a hydrogen bond from the molecule. Above 2 eV carbon reflection is in the form of complex hydrocarbon emission with two or three carbon atoms. Also the reflection coefficient increases as the hybridization changes from  $sp$  to  $sp^3$ .  $C_2H_x$  ( $x = 1-6$ ) have higher reflection coefficient for an even number of hydrogen atoms and a lower reflection coefficient for odd number of hydrogen atoms. Above 1 eV hydrogen capture or break-up is dominant in the reflection pattern. With increasing energy more than one hydrogen atom or carbon–carbon bond break-up is observed. The energy dependence of the reflection coefficient is used in the ERO modeling of PSI-2 [10].

#### References

- [1] W. Jacob, J. Nucl. Mater. 337–339 (2005) 839.
- [2] G. Federici, C.H. Skinner, J.N. Brooks, J.P. Goad, C. Grisolia, et al., Nucl. Fus. 41 (2001) 1967.
- [3] J.P. Goad, N. Bekris, J.D. Elder, S.K. Erents, D.E. Hole, et al., J. Nucl. Mater. 290–293 (2001) 224.
- [4] M. Mayer, V. Philipps, P. Wienhold, H.G. Esser, J. von Seggern, et al., J. Nucl. Mater. 290–293 (2001) 381.
- [5] V. Rohde, M. Mayer, ASDEX Upgrade Team, J. Nucl. Mater. 313–316 (2003) 337.
- [6] V. Rohde, M. Mayer, ASDEX Upgrade Team, Physica Scripta T103 (2003) 25.
- [7] M. Mayer, V. Rohde, A. von Keudell, ASDEX Upgrade Team, J. Nucl. Mater. 313–316 (2003) 429.
- [8] M. Mayer, V. Rohde, J. Likonen, E. Vainonen-Ahlgren, K. Krieger, et al., J. Nucl. Mater. 337–339 (2005) 119.
- [9] W. Bohmeyer, D. Naujoks, A. Markin, I. Arkhipov, B. Koch, et al., J. Nucl. Mater. 337–339 (2005) 89.
- [10] W. Bohmeyer, A. Markin, D. Naujoks, B. Koch, G. Krenz, these Proceedings, doi:10.1016/j.jnucmat. 2007.01.163.

- [11] A.B. Erhardt, W.D. Langer, Technical Report PPPL-2477, Princeton Plasma Physics Laboratory, 1987.
- [12] D. Alman, D.N. Ruzic, Phys. Plasmas 7 (2000) 1421.
- [13] J.N. Brooks, Z. Wang, D.N. Ruzic, D.A. Alman, Technical Report ANL/FPP/TM-297 REV, Argonne National Lab, 1999.
- [14] R.K. Janev, D.D. Reiter, Technical Report Jul3966, Forschungszentrum Jülich, Jülich, 2002.
- [15] D. Naujoks, D. Coster, H. Kastelewicz, R. Schneider, J. Nucl. Mater. 266–269 (1999) 360.
- [16] D. Naujoks, Physica Scripta 111 (2004) 80.
- [17] D.W. Brenner, Phys. Rev. B 42 (1990) 9458.
- [18] P. Traskelin, E. Salonen, K. Nordlund, J. Keinonen, C.H. Wu, J. Nucl. Mater. 334 (2004) 65.
- [19] A. Pospieszczyk, G. Sergienko, D. Rusbuldt, Contrib. Plasma Phys. 40 (2000) 162.
- [20] J. Hiskes, Bull. Am. Phys. Soc. 25 (1980) 981.
- [21] J. Hiskes, Appl. Phys. Lett. 57 (1990) 231.
- [22] G. Stutzin, A. Young, A. Schlachter, K. Leung, W. Kunkel, Chem. Phys. Lett. 155 (1989) 475.
- [23] G. Stutzin, A. Young, H. Dobeles, A. Schlachter, K. Leung, et al., Rev. Sci. Instrum. 61 (1990) 619.
- [24] P. Eenshuistra, J. Bonnie, J. Los, H. Hopman, Phys. Rev. Lett. 60 (1988) 341.
- [25] P. Eenshuistra, R. Heeren, A. Kleyn, H. Hopman, Phys. Rev. A 40 (1989) 3613.
- [26] D. Marx, M. Parrinello, Science 271 (1996) 179.
- [27] Z. Vager, D. Zaffman, T. Graber, E.P. Ranter, Phys. Rev. Lett. 71 (1993) 4319.
- [28] B.J. Braams, C. Chen, X. Huang, Z. Jin, Z. Xie, et al., 231st ACS National Meeting, Atlanta, GA, March 26–30 Phys. 433, 2006.
- [29] D. Alman, D.N. Ruzic, Physica Scripta T111 (2004) 145.
- [30] A.R. Sharma, R. Schneider, U. Toussaint, K. Nordlund, Hydrocarbon radicals interaction with amorphous carbon surface, <http://www.ipp.mpg.de>, 2006.